NANO
LETTERS

2007
Vol. 7, No. 11
3489−3492

Nanoscale γ-AlO(OH) Hollow Spheres: Synthesis and Container-Type Functionality

Daniel H. M. Buchold and Claus Feldmann*

Institute of Inorganic Chemistry, University of Karlsruhe (TH), Engesserstrasse 15, D-76131 Karlsruhe, Germany

Received August 17, 2007; Revised Manuscript Received October 10, 2007

ABSTRACT

AlO(OH) hollow spheres are realized via a water-in-oil (w/o) microemulsion, applying the liquid-to-liquid-phase boundary of the micellar system as a template. Scanning electron microscopy, transmission electron microscopy (TEM), and dynamic light scattering analyses show the presence of nonagglomerated hollow spheres exhibiting an outer diameter of about 30 nm and a wall thickness of 5–6 nm. High-resolution TEM images show highly ordered lattice fringes, indicating the crystallinity of the sphere wall and identifying the wall to consist of γ-AlO(OH) (boehmite). The container functionality of as-prepared AlO(OH) hollow spheres is validated as a proof of concept by encapsulating the fluorescent dye rhodamine (R6G) inside the alumina shell. Subsequent to centrifugation and careful purification, R6G is evidenced via photoluminescence to be still present. Finally, release of R6G is initiated by acidic dissolution of the sphere wall.

Advanced nanostructured materials are of fundamental interest to chemistry and materials science.[1] Among them hollow spheres gained significant importance in recent years as well. Several types of applications such as container-type functionalities including controlled molecule release or drug delivery, high-surface materials for catalysis, or gas adsorption and structural building units for ultrasonic imaging or for low-weight materials have been intensely discussed already.[2] Hollow spheres with different compositions (e.g., SiO_2, ZrO_2, GaN, Au, Pt, CoPtPd, various polymers, and polyelectrolytes) have been predominately realized on the mesoscale ($Ø_{sphere} > 100$ nm).[3] On the nanoscale ($Ø_{sphere} < 100$ nm), compounds such as Al_2O_3, LaF_3, Co_9S_8, Ag, Au, or Pd are still available.[4]

The most common strategy to realize nanoscale hollow spheres is based on a solid core on which as a first step a shell is precipitated. As a second step, the core/template is removed by a suited etching process. This strategy requires monodispersed and nonagglomerated templates, for instance, colloidal polymer lattices, silica, or gold particles.[4] The solid template, however, to some extent can be disadvantageous, for example, with concern to the removal of the template without destructing the shell or regarding the refilling of the sphere interior by means of container-type funtionalities. Such container functionalities have been intensely studied with polyelectrolyte capsules.[5] Here, incorporation/release of molecules or drugs is most often performed with meso- to micron-scaled shells by changing the osmotic pressure. Such a behavior has not been shown with nanoscale hollow spheres and can be expected to be more difficult in the case of inorganic spheres, for instance, due to a limited elasticity of inorganic materials as well as stronger capillary forces.

As an alternative approach to solid templates, the water droplets of micellar systems also may function as a template. On the basis of the well-established size control of micelles and the possiblity to dissolve all kinds of ingredients (e.g., salts, molecules) in the micell prior to establishing and closing the shell, such liquid templates would offer a wide adaptability with respect to synthesis and application. Indeed, such a microemulsion approach has been discribed already. Here, hollow spheres with comparably broad size distribution have been aggregated to form zeolith-type, microporous solids exhibiting large specifc surfaces.[6] Further investigations have also been directed to mesoscaled spheres ($Ø_{sphere} > 100$ nm).[7] By means of fundamental materials science as well as by applicational aspects (e.g., thin layers, filler material, biomedical purposes), however, nonagglomerated and nanoscale spheres are requested. Such materials surprisingly have been barely verified via a microemulsion-based approach.[8] Crystalline, nonagglomerated and nanoscale γ-AlO(OH), boehmite, is here first presented as a nanoscale hollow sphere.

In this study, the micellar system was established by dissolving 0.91 g cetyltrimethylammonium bromide (CTAB) as a surfactant and 2.5 mL of 1-hexanol as a cosurfactant in 25.0 mL of *n*-dodecane as the nonpolar oil-phase. To this

---

* Corresponding author. Fax: (+)49-721-6084892. E-mail: feldmann@aoc1.uni-karlsruhe.de.

10.1021/nl072074f CCC: $37.00

Scheme 1. Scheme Illustrating the Course of Reaction: (A) Micellar System with Reactants; (B) Formation of AlO(OH) Sphere; (C) Acidic Dissolution of Sphere Wall

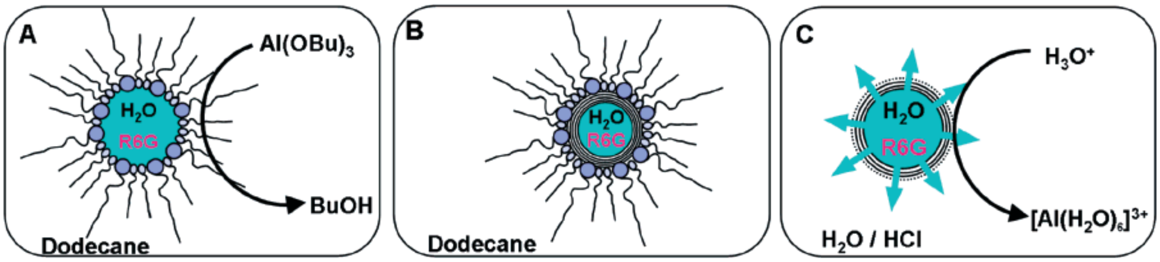

micellar system, a mixture of 0.5 mL of H_2O and 0.5 mL of methanol as the polar phase was added at ambient temperature (20 °C). Finally, 2.0 mL of 1.0 M $Al(sec\text{-}OC_4H_9)_3$/dodecane solution was added under vigorous stirring to the equilibrated, transparent water-in-oil (w/o) microemulsion (Scheme 1A). Immediately after admixing of the alkoxide, stirring was stopped, and the micellar system was left to react for 12 h. Within this equilibrated and nonstirred micellar system, hydrolysis of the aluminum alcoholate occurs at the liquid-to-liquid-phase boundary (Scheme 1B). The selection of the aluminum alcoholate, considering first a slow diffusion-controlled hydrolysis and second a solubility being much higher in the nonpolar phase compared to the polar phase, turned out to be prerequisite to the underlying course of reaction.

To separate the solid material from the micellar system, they are most often destabilized by the addition of polar, aprotic solvents (e.g., acetone).[9] With this measure, a certain agglomeration of the destabilized particles always occurs and is denoted to be a drawback of microemulsion techniques.[10] In contrast, the reaction was terminated here upon the addition of 10 mL of diethylene glycol (DEG) to the micellar system.[11] This resulted in an immediate phase separation with a top phase, which mainly consists of dodecane and CTAB, and a DEG bottom phase containing the far most of the AlO(OH) spheres. DEG is also known to efficiently stabilize the particle surfaces.[12] As a consequence, the AlO(OH) spheres could easily be redispersed in DEG or water. With an average value of 33 nm, dynamic light scattering (DLS) confirms the particle diameter observed with electron microscopy and shows the absence of agglomerates (Figure 1). From the DEG suspension, the hollow spheres can also be collected by centrifugation as a colorless powder.

Electron microscopy elucidates morphology and size of the hollow spheres (Figure 2). Scanning electron microscopy (SEM) images show a variety of nonagglomerated particles, exhibiting a diameter of about 30 nm (Figure 2A). The presence of hollow spheres is evidenced by transmisstion electron microscopy (TEM) images (Figure 2B). Partial destruction of as-prepared spheres due to evacuation of the liquid-filled spheres as well as due to electron bombardment of the nonconducting sphere walls, which was observed quite often under TEM conditions,[13] is reduced successfully by careful drying and evacuation (12 h at 60 °C). The different contrast of the displayed particles can be attributed to their different orientation relative to the electron beam. High-resolution TEM (HRTEM) images show ellipsoidal particles with outer diameters of about 20 nm (short axis) and 35 nm (long axis) and a wall thickness of 4.5−6.5 nm (Figure 2C). The ellipsoidal appearance of the particles again is attributed to a vacuum-induced deformation of the formerly liquid-filled spheres. HRTEM images also exhibit highly ordered lattice fringes, indicating the crystallinity of the sphere wall (Figure 2C). The d-value of 3.2 Å corresponds well with the presence of γ-AlO(OH) (boehmite, (120) lattice plane with 3.17 Å).[14] In addition, chemical composition and crystallinity of γ-AlO(OH) are confirmed by electron diffraction patterns (Figure 2D) as well as X-ray diffraction patterns (see Supporting Information). Taking into account that the synthesis is carried out at ambient temperature (20 °C), the crystallinity of the sphere wall, which is observed for all spheres investigated, is even more surprising.

The container-type functionality of the γ-AlO(OH) spheres was verified as a proof of concept by adding the fluorescent dye rhodamine (R6G) to the polar phase (Scheme 1A). To this end, R6G was selected due to its intense emission, which allows a definite detection via fluorescence spectroscopy even in very low concentrations. To fill the spheres, the synthesis was performed as described, applying 0.5 mL of 10^{-7} M R6B solution instead of pure water. With the formation of the alumina shell, the dye was encapsulated (Scheme 1B). The R6G-filled AlO(OH) spheres were then separated by centrifugation. On a time scale of separation and washing (30−60 min), R6G remaining in the supernatant was only

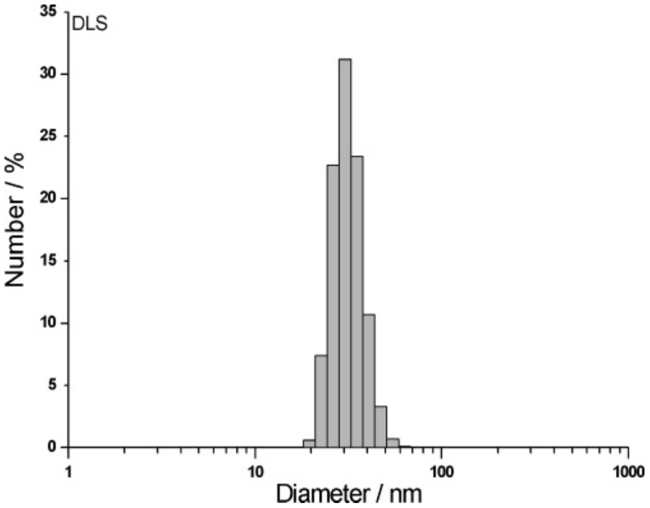

Figure 1. Particle size distribution of hollow AlO(OH) after separation from the microemulsion, purification, and redispersion in diethylene glycol.

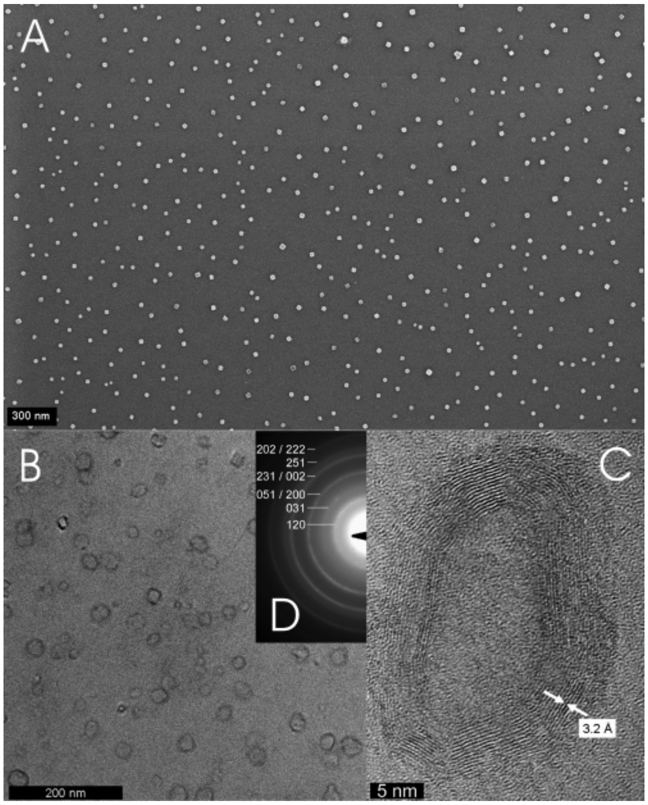

Figure 2. Electron microscopy of as-prepared AlO(OH): (A) SEM and (B) TEM micrographs indicating the uniformity of the particles; (C) HR-TEM micrograph showing lattice fringes; and (D) electron diffraction pattern with Miller indices of γ-AlO(OH)/boehmite.[14]

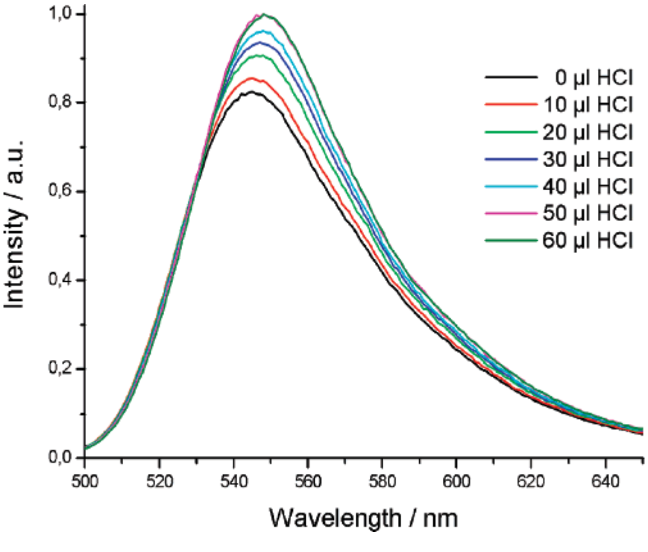

Figure 3. Photoluminescence of R6G-filled AlO(OH) spheres suspended in water, recorded during acidic dissolution ($\lambda_{\text{excitation}}$ = 480 nm).

detected subsequent to this very first centrifugation (control via photoluminescence). To remove all constituents of the micellar system, the as-prepared solid was carefully purified, twice by resuspension and centrifugation with isopropyl alcohol and twice by resuspension and centrifugation with water. Finally, the spheres were resuspended in water. Photoluminescence shows R6G still to be present (Figure 3).

Scheme 2. Scheme Displaying the Optical Conditions for Excitation (λ_{ex} = 480 nm) and Emission (λ_{em} = 550 nm) of R6G-filled AlO(OH) Spheres (A, Absorbed Light; R, Reflected Light; T, Transmitted Light)

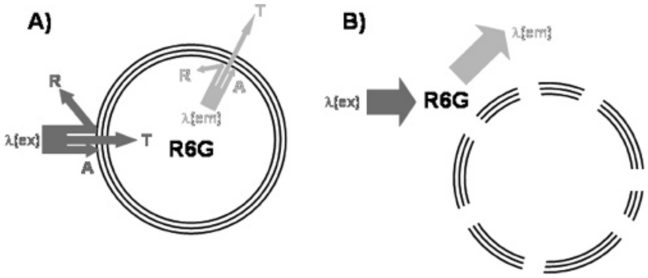

Controlled release of R6G was initiated by HCl-driven dissolution of AlO(OH) (Scheme 1C). To this concern, concentrated hydrochloric acid (32%) was added with a microliter injection syringe in portions of 10 μL to 4 mL of an aqueous suspension containing 8 mg of AlO(OH) spheres. The course of reaction was followed by photoluminescence, which was recorded by excitation at 480 nm and corrected for the wavelength-dependent response of the spectrometer. Obviously, an increase in photoluminescence is observed up to the addition of about 30 μL of HCl (Figure 3). This finding is in accordance with a certain absorption and reflection of excited as well as emitted light due to the intact sphere wall (Scheme 2). With the proceeding dissolution of AlO(OH), R6G diffuses out of the sphere, then absorbs all incoming light, and therefore leads to an increase in photoluminescence. To this end, DLS analysis indeed shows complete dissolution of AlO(OH) to require about 60 μL of HCl. Obviously, acidic dissolution at an early point in time results in sphere leakages. Considering that etching at ambient conditions (20 °C) would proceed preferentially at reactive surface sites, such an effect is to be expected.[15] During the acid-driven R6G release, the pH-level of the suspension ranged from 8.2 (virgin AlO(OH) suspension) to 5.8 (release of R6G completed) and was then further decreased with the proceeding formation of the acidic complex $[Al(H_2O)_6]^{3+}$.

For further validation of R6G release, photoluminescence was compared to two references: A, an aqueous solution of

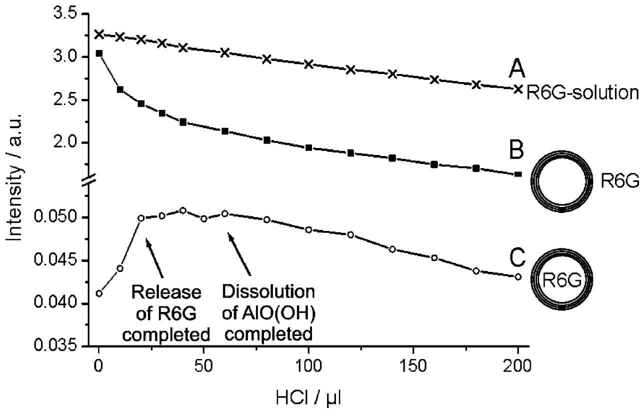

Figure 4. Course of the rhodamine 6G photoluminescence intensity upon addition of hydrochloric acid. (A) solution of R6G; (B) suspension of AlO(OH) hollow spheres with R6G added to the outside of the spheres; (C) R6G-filled AlO(OH) hollow spheres.

R6G (10^{-7} M) and B, nonfilled AlO(OH) hollow spheres (2 mg/mL), which were suspended in aqueous R6G solution (10^{-7} M) (Figure 4). The photoluminescence intensity in each case was calculated by mathematical fitting of the peak area of the relevant emission spectra. In contrast to R6G-filled spheres (Figure 4, case C), for A and B emission decreases linearly with the addition of HCl. This is due to well-known acidic quenching of R6G photoluminescence.[16] With R6G released out of the AlO(OH) sphere, quenching was also found for C. When adding more than 60 μL of HCl, the photoluminescence of C is in parallel to A and B finally. Both effects, the increase in photoluminescence for C at first and the significantly different behavior in comparison to A and B, clearly show the container-type functionality of γ-AlO(OH) hollow spheres.

Acknowledgment. The authors are grateful to W. Send and Professor Dr. D. Gerthsen for performing TEM analysis. We also acknowledge the Center for Functional Nanostructures (CFN) of the Deutsche Forschungsgemeinschaft (DFG) at the University of Karlsruhe (TH).

Supporting Information Available: A detailed description of the microemulsion-based synthesis as well as a detailed description of the analytical characterization, also including X-ray diffraction patterns. This material is available free of charge via the Internet at http://pubs.acs.org.

References

(1) (a) Ozin, G. A.; Arsenault, A. C. *Nanochemistry*; RSC Publishing: Cambridge, 2005; pp 167. (b) Kumar, S.; Nann, T. *Small* **2006**, *2*, 316. (c) Zhao, L.; Yosef, M.; Pippel, E.; Hofmeister, H.; Steinhart, M.; Gösele, U.; Schlecht, S. *Angew. Chem., Int .Ed.* **2006**, *45*, 8042. (d) Remskar, M. *Adv. Mater.* **2004**, *16*, 14.

(2) (a) Hainfeld, J. F.; Slatkin, D. N.; Focella, T. M.; Smilowitz, H. M. *Br. J. Radiol.* **2006**, *79*, 248. (b) Mufti, J.; Cernasov, D.; Macchio, R. *Household Pers. Prod. Ind.* **2002**, *39*, 75. (c) Storhoff, J. J.; Elghanion, R.; Mucic, R.; Mirkin, C. A.; Letsinger, R. L. *J. Am. Chem. Soc.* **1998**, *120*, 1959. (d) Dössel, O. *Bildgebende Verfahren in der Medizin*; Springer: Berlin, 2000. (e) Andersen, O.; Waag, U.; Schneider, L.; Stephani, G.; Kieback, B. *Adv. Eng. Mater.* **2000**, *2*, 192.

(3) (a) Arnal, P. M.; Comotti, M.; Schüth, F. *Angew. Chem., Int. Ed.* **2006**, *45*, 8224. (b) Djojoputro, H.; Zhou, X. F.; Qiao, S. Z.; Wang, L. Z.; Yu, C. Z.; Lu, G. Q. *J. Am. Chem. Soc.* **2006**, *128*, 6320. (c) Lou, X. W.; Wang, Y.; Yuan, C.; Lee, J. Y.; Archer, L. A. *Adv. Mater.* **2006**, *18*, 2325. (d) Zhang, X.; Li, D. *Angew. Chem., Int. Ed.* **2006**, *45*, 5971. (e) Lou, X. W.; Yuan, C.; Zhang, Q.; Archer, L. A. *Angew. Chem., Int. Ed.* **2006**, *45*, 3825. (f) Liu, J.; Maaroof, A. I.; Wieczorek, L.; Cortie, M. B. *Adv. Mater.* **2005**, *17*, 1276. (g) Sun, X.; Li, Y. *Angew. Chem., Int. Ed.* **2004**, *43*, 3827. (h) Shchukin, D. G.; Sukhorukov, G. B.; Möhwald, H. *Angew. Chem., Int. Ed.* **2003**, *42*, 4472.

(4) (a) Ras, R. H. A.; Kemell, M.; de Witt, J.; Ritala, M.; ten Brinke, G.; Leskelä, M.; Ikkala, O. *Adv. Mater.* **2007**, *19*, 102. (b) Yin, Y.; Erdonmez, C. K.; Cabot, A.; Hughes, S.; Alivisatos, A. P. *Adv. Funct. Mater.* **2006**, *16*, 1389. (c) Sun, Y.; Xia, Y. *J. Am. Chem. Soc.* **2004**, *126*, 3892. (d) Selvakannnan, P.; Sastry, M. *J. Chem. Soc., Chem. Commun.* **2005**, 1684. (e) Xiong, Y.; Wiley, B.; Chen, J.; Li, Z. Y.; Yin, Y.; Xia, Y. *Angew. Chem., Int. Ed.* **2005**, *44*, 7913. (f) Liu, R.; Dong, P.; Chen, S. L. *Chem. Lett.* **2005**, *34*, 548. (g) Wang, X.; Li, Y. *Angew. Chem., Int. Ed.* **2003**, *42*, 3497.

(5) (a) Johnston, A. P. R.; Cortez, C.; Angelatos, A. S.; Caruso, F. Caruso, *Curr. Opin. Colloid Interface Sci.* **2006**, *11*, 203. (b) Peyratout, C. S.; Dähne, L. *Angew. Chem., Int. Ed.* **2004**, *43*, 3762.

(6) (a) Fumihiro, H.; Shoju, M. Patent application, JP 2007044610. (b) Fujiwara, M.; Shiokawa, K.; Sakakura, I.; Nakahara, Y. *Nano Lett.* **2006**, *6*, 2925. (c) Yasuyuki, O.; Seiji, S. Patent application, JP 4250842. (d) Koetz, J.; Abetz, V.; Lutter, S. Patent application, DE 102005035374. (e) Jafelicci, M.; Davalos, M. R.; Dos Santos, F.; De Andrade, S. J. *J. Non-Cryst. Solids* **1999**, *247*, 98.

(7) (a) Lu, J.; Chen, D.; Jian, X. *J. Colloid Interface Sci.* **2006**, *303*, 437. (b) Sgraja, M.; Bertling, J.; Kümmel, R.; Jansens, P. J. *J. Mater. Sci.* **2006**, *41*, 5490. (c) Wu, D.; Ge, X.; Zhang, Z.; Wang, M.; Zhang, S. *Langmuir* **2004**, *20*, 5192. (d) Shchukin, D. G.; Sukhorukov, G. B. *Adv. Mater.* **2004**, *16*, 671.

(8) (a) Liu, Q.; Liu, H.; Hin, M.; Zhu, J.; Liang, Y.; Xu, Z.; Song, Y. *Adv. Mater.* **2005**, *17*, 1995. (b) Ni, Y.; Tao, A.; Hu, G.; Cao, X.; Wei, X.; Yang, Z. *Nanotechnology* **2006**, *17*, 5013. (c) Zimmerman, C.; Wanner, M.; Gerthsen, D.; Feldmann, C. *Small* **2007**, *3*, 1347.

(9) (a) Dwars, T.; Paetzold, E.; Oehme, G. *Angew. Chem., Int. Ed.* **2005**, *44*, 7174. (b) Cushing, B. L.; Kolesnichenko, V. L.; O’Connor, C. J. *Chem. Rev.* **2004**, *104*, 3893. (c) Dörfler, H. D. *Grenzflächen und kolloiddisperse Systeme*; Springer: Berlin, 2003.

(10) Lee, Y.; Lee, J.; Bae, C. J.; Park, J. G.; Noh, H. J.; Park, J. H.; Hyeon, T. *Adv. Funct. Mater.* **2005**, *15*, 503.

(11) Buchold, D. H. M.; Feldmann, C. *Chem. Mater.* **2007**, *19*, 3376.

(12) (a) Feldmann, C.; Jungk, H. O. *Angew. Chem., Int. Ed.* **40** (2001) 359. (b) Feldmann, C. *Adv. Funct. Mater.* **13** (2003) 101.

(13) (a) Smith, D. J.; Petford-Long, A. K.; Wallenberg, L. R.; Bovin, J.-O. *Science* **1986**, *233*, 872. (b) Ajayan, P. M.; Marks, L. D. *Phys. Rev. Lett.* **1988**, *60*, 585., (c) Williams, P. *Appl. Phys. Lett.* **1987**, *50*, 1760.

(14) Christensen, A. N.; Lehmann, M. S.; Couvert, P. *Acta Chem. Scand. A* **1982**, *36*, 303.

(15) Myers, D. *Surfaces, Interfaces and Colloids*; Wiley-VCH: New York, 1999; p 125.

(16) (a) *Industrial Dyes*; Hunger, K., Ed.; Wiley-VCH: Weinheim, 2002. (b) Levshin, L. V.; Mittsel, Y. A.; Nizamov, N. *Zh. Prikl. Spek.* **1969**, *10*, 509.

NL072074F